Ising on $\mathbb{S}^2$ - The Affine Conjecture

Richard C. Brower,[a,*] **George T. Flemming,**[b] **Nobuyuki Matsumoto**[a] **and Rohan Misra**[a]

[a]*Boston University, Boston, MA 02215, USA*

[b]*Fermi National Accelerator Laboratory, Batavia, Illinois, 60510, USA*

E-mail: brower@bu.edu

We review the recent construction [1] of the 2d Ising model on a triangulated sphere $\mathbb{S}^2$. Surprisingly, this led to a precise map of the lattice couplings to the target geometry in order to reach the conform field theory (CFT) in the continuum limit. For the integrable 2d Ising CFT, the map was found analytically [2]. Here we conjecture how this might be generalized. The discrete geometry is implemented by the piecewise flat triangulation introduced by Regge in 1960 for the Einstein Hilbert action [3]. Then following our Ising example, we posit the existence of a smooth map of lattice couplings in affine parameters consistent with quantum correlators. A sequence of theoretical investigations and numerical simulations are recommended to test this conjecture. They begin with non-integrable CFT's – the 2d ϕ^4 theory on $\mathbb{S}^2$; the 3d Ising model on $\mathbb{S}^3$ and $\mathbb{R} \times S^2$; QED3 on $\mathbb{R} \times \mathbb{S}^2$ as an intermediate step to 4d non-Abelian lattice gauge theory on $\mathbb{R} \times \mathbb{S}^3$.

The 41st International Symposium on Lattice Field Theory (LATTICE2024)
28 July - 3 August 2024
Liverpool, UK

---

*Speaker

1. Introduction

The Monte Carlo simulations of the Euclidean path integral in flat space on hypercubic lattices have proven to be a powerful *ab initio* solutions to non-perturbative field theory as exemplified by lattice QCD. Extending these to lattice field theory on curved manifolds could open up a new area of investigation for non-perturbative quantum field theory. In 1985, Cardy [4] already emphasized the advantage for conformal field theory (CFT) of radial quantized lattice on $\mathbb{R} \times S^{d-1}$, with the warning of the formidable challenge of spherical lattices for d >2. The Quantum Finite Element (QFE) project has taken on this task, beginning with the Ising CFT or the universally equivalent ϕ^4 theory. In 2d the stereographic projection to the Riemann sphere, $\mathbb{R}^2 \to \mathbb{S}^2$, is a useful first step to implementing spherical lattices, with advantage comparison to the exact solution to the $c = 1/2$ minimal model. Development of QFE project is given in a sequence of publications [1, 2, 5–8]. However in this talk, technical details are avoided to provide a heuristic narrative to our conjecture.

2. Classical Field Limit

We begin with the classical action for ϕ^4 theory on a curved Euclidean manifold,

$$S_M = \frac{1}{2} \int_{\mathcal{M}} d^d x \sqrt{g} [g^{\mu\nu}(x) \partial_\mu \phi(x) \partial_\nu \phi(x) + \xi_0 \mathbf{R} + m^2 \phi^2(x) + \lambda \phi^4(x)] \ . \tag{1}$$

Perturbative renormalization has been extensively studied for this example [9]. Placing this on a lattice, requires introducing a graph, assigning the metric ($g_{\mu\nu}(x)$) and field ($\phi(x)$) to sites $i = 1, .., N$ and directed links $\langle i, j \rangle$:

$$S_{FEM} = \frac{1}{2} \sum_{\langle i,j \rangle} K_{ij}(\phi_i - \phi_j)^2 + \frac{1}{2} \sum_i \sqrt{g_i} [\mu_0^2 \phi_i^2 + \lambda_0 (\phi_i^2 - 1)^2]] \ . \tag{2}$$

We dropped the Ricci scalar $\mathbf{R}$ which decouples in $2d$ but plays an important role in $3d$ [7, 8]. On the graph, all bare parameters are dimensionless. The shift in bare mass parameter, $m_0^2 = \mu_0^2 - 2\lambda_0$, gives a simple parameterization in the bare coupling λ_0 between the free CFT at $\lambda_0 = 0$ to the Ising model at $\lambda_0 = \infty$.

2.1 The Regge Simplicial Manifold

At the classical level, a single framework between geometry and matter is provided by the Einstein Hilbert action,

$$S = S_{EH} + S_M = \int dx \sqrt{g} \left[\frac{1}{2\kappa}(R - 2\Lambda) + \mathcal{L}_M \right] \ , \tag{3}$$

and its equation of motion (EOM),

$$\frac{\delta S}{\delta g^{\mu\nu}(x)} \implies R_{\mu\nu}(x) - \frac{1}{2} g_{\mu\nu}(x) R(x) - \Lambda g_{\mu\nu}(x) = \kappa T_{\mu\nu}(x) \ . \tag{4}$$

To discretize the manifold we note that Whitney's embedding theorem states that any smooth d-dimensional manifold has an isometric embedding in $\mathbb{R}^{2d}$. So Regge approximates the manifold by
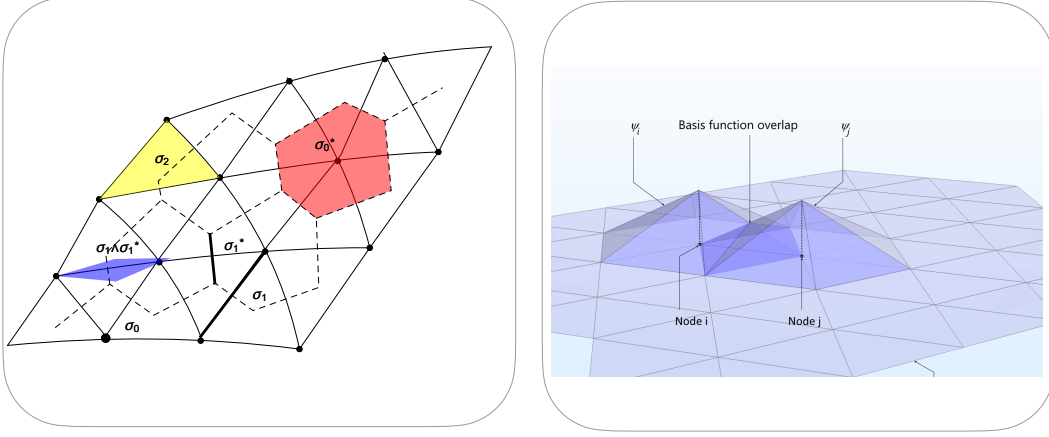
Figure 1: On the left is portion of 2d Regge simplicial manifold composed triangular 2 simplices, $\sigma_2(ijk)$, joined a boundary edges with length, $|\sigma_1(ij)| = \ell_{ij}$, and dual distances, $\sigma_1^*(ij) = \ell_{ij}^*$, between circumcenter dual sites. On right FEM linear basis element for a scaler field ϕ_i.

a set flat planes intersecting the surface, forming d-simplices σ_d: triangles in 2d, tetrahedron in 3d etc. This same manifold on the left in Fig.1, when used to discretize classical equation, is referred to as the Finite Element Method (FEM) illustrated on the right in Fig 1.

The simplices share boundaries to form a continuous manifold. The entire geometry is encoded in the flat interiors of each simplex, $\sigma_d(0, 1, .., d)$, with vertices at $\vec{r}_i$ in $\mathbb{R}^d$. The $d(d + 1)/2$ edge lengths, $\ell_{ij} = |r_i - r_j|$, determine the affine subspace. The metric field is replaced by $g_{\mu\nu}(x) \rightarrow \{\ell_{ij}\}$. The curvature is isolated to $d-2$ dimensional delta functions on hinges weighted by hing volumes, V_h, and the total deficit angle, ϵ_h, from the sum of dihedral angles contributing to the hing, $h \in \sigma$, as illustrated for 3d in Fig 2. Integrating the Enstein-Hilbert action yields Regge's calculus action [3],

$$S_{Regge}[\ell_{ij}] = \sum_h V_h \epsilon_h - 2\Lambda \sum_{\sigma_d} |\sigma_d| \quad \text{with} \quad \epsilon_h = 2\pi - \sum_{h \in \sigma} \theta_{\sigma,h} \,, \tag{5}$$

and the equations of motion,

$$\frac{\partial S_{Regge}}{\partial \ell_{ij}} = \sum_h \frac{\partial V_h}{\partial \ell_{ij}} \epsilon_h + \sum_h V_h \cancelto{0}{\frac{\partial \epsilon_h}{\partial \ell_{ij}}} - 2\Lambda \sum_{\sigma_d \supset \ell_{ij}} \frac{\partial |\sigma_d|}{\partial \ell_{ij}} = 0 \,. \tag{6}$$

The second term in the middle is exactly zero due the Schläfli identity [10]. The is a mathematically elegant FEM discretization [11] with discrete curvature tensors, Bianchi identities [12–14] etc. With positive cosmological constant, Ricci flow [15] converges to spherical manifolds. Apparently the Regge 3d manifold also helped to illuminate the proof of the Poincaré conjecture [16, 17] that there is unique manifold homeomorphic to $\mathbb{S}^3$.

Turning to the scalar field theory in 2d, the weights in Eq. 2 on edge $\langle i, j \rangle$ are given by

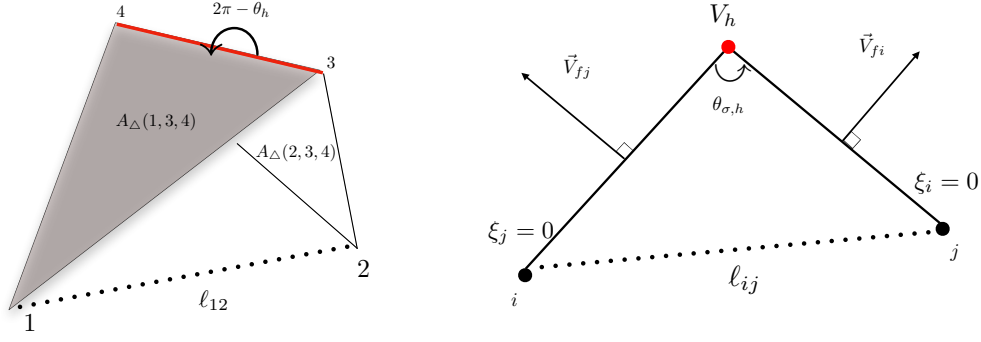$$K_{ij} = \frac{\ell_{ij}^*}{\ell_{ij}} \tag{7}$$

Figure 2: On the left, a tetrahedral simplex with a dihedral angle, $\theta_{\sigma,h}$, on the hing at the edge $\langle 3, 4 \rangle$ at the intersection of two triangles. On the right the hing for a d-simplex occupies a $d-2$ dimensional volume, V_h. The dihedral angle is defined by a scalar product between vectors normal to $d-1$ faces $\vec{V}_{fi}, \vec{V}_{fj}$ at $\xi_i = 0, \xi_j = 0$ respectively.

using piecewise linear FEM, where ℓ_{ij}^* are distance on the circumcenter dual lattice.

For a simple example of the intimate relation between the Regge's geometry and linear finite elements, we now sketch the computation of kinetic term (7) for $d \geq 2$. The central trick is to introduce barycentric co-ordinates, ξ_i, both for the interior of a d-simplex, $\sigma_d(0, 1, ..., d)$, with $\xi_k \leq 0$ and $\xi_0 + \xi_1 + \cdots + \xi_d = 1$ and for linear interpolation field values: $\phi_i = \phi(\vec{r}_i)$ at the sites $\vec{r}_i$:

$$\vec{x} = \xi^0 \vec{r}_0 + \xi^1 \vec{r}_1 + \cdots + \xi^d \vec{r}_d \quad , \quad \phi(x) = \xi^0 \phi_0 + \xi^1 \phi_1 + \cdots + \xi^d \phi_d \tag{8}$$

Changing variables in the integral yields simplex we compute the simplex contribution to the edges weights,

$$\int_{\sigma_d} d^d x \sqrt{g} g^{\mu\nu} \partial_\mu \phi(x) \partial_\mu \phi(x) \quad \Longrightarrow \quad K_{ij}^{\sigma_d} = -|\sigma_d| \vec{\nabla} \xi^i \cdot \vec{\nabla} \xi^j = \frac{\vec{V}_{f_i} \cdot \vec{V}_{f_j}}{d^2 |\sigma_d|} = \frac{\partial V_d}{\partial \ell_{ij}^2} . \tag{9}$$

The FEM kinetic term is geometrized as the derivative of the volume $V_d = |\sigma_d|$ with respect to the edge conjugate to the hinge! A slight generalization gives the energy momentum tensor as well. The trace matches the cosmological term. This is just a taste of the remarkable identities. For the free CFT ($\lambda_0 = 0$) Regge plus FEM is a complete solution – both the geometry and the field extrapolate to exact continuum theory in the limit $\ell_{ij} < a$ as $a \to 0$. **Now our task is to find a way to transfer this simplicial geometry to lattice quantum field theory correlators.**

2.2 Affine Space

The affine geometry plays a key role in our generalization. In $\mathbb{R}^d$ the affine transformation is general linear map,

$$x^\mu = A_{\mu,i} \xi^i + b^\mu \quad \text{or} \quad \vec{x} = \vec{e}_i \xi_i + \vec{b} \tag{10}$$

extending the $d(d+1)/2$ Poincare generators by a factor of 2 to a total of $d(d+1)$ generators. The additional parameters represent a constant affine metric,

$$ds^2 = d\vec{x} \cdot d\vec{x} = (A^T A)_{ij} d\xi^i d\xi^j = g_{ij} d\xi^i d\xi^j \quad \Longrightarrow \quad g_{ij} = \vec{e}_i \cdot \vec{e}_j; . \tag{11}$$

Each simplex is affine equivalent of a standard equilateral simplex with unit edge length. For 2d $d(d+1)/2 = 3$ the triangle edges lengths, $\ell_{12}, \ell_{23}, \ell_{31}$ represent scale (similarity) plus shape. In 3d the tetrahedron has a 6 affine edge lengths, the 4-plex 10 edge lengths, etc. Regge constructs the simplicial geometry by gluing the affine subspaces into a piecewise linear manifold. We also anticipate that a global affine transformation for lattice field correlators at t the critical point takes circle(spheres) to ellipse (ellipsoids). For 2d, this was proven

$$\langle \phi(x,y)\phi(0,0)\rangle = \frac{1}{(x^2+y^2)^{\Delta_\phi}} \longrightarrow \frac{1}{(ax^2+by^2+cxy)^{\Delta_\phi}} \, , \tag{12}$$

for the general triangular Ising model ([2]).

3. Ising model on a 2-sphere

In Ref [2] on the *Ising Model on the Affine Plane* , we gave an analytical solution to the general triangular Ising model with 3 couplings K_1, K_2, K_3. The solution follows from the star-triangle
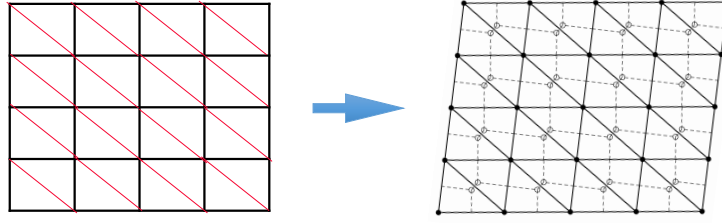

Figure 3: On the square lattice Ising model, $S_\square = -K(s_i s_{i+\hat{1}} + s_i s_{i+\hat{2}})$, on the left is generalized to a regular triangular graph, $S_\triangle = -K_1 s_i s_{i+\hat{1}} - K_2 s_i s_{i+\hat{2}} - K_3 s_i s_{i+\hat{3}}$ with 3 couplings.

relation, the Kramers-Wannier map to hexagonal lattice and the use free Wilson-Majorana fermions as describe by Wolff in Ref. [18]. To restore spherical symmetry in $\mathbb{R}^2$ the metric map along 3 oblique co-ordinate is

$$\sinh(2K_1) = \frac{\ell_1^*}{\ell_1} \quad , \quad \sinh(2K_2) = \frac{\ell_2^*}{\ell_2} \quad , \quad \sinh(2K_3) = \frac{\ell_3^*}{\ell_3} \tag{13}$$

The 3 scale-invariant equations implying the constraint to the 2d critical surface,

$$p_1 p_2 + p_2 p_3 + p_3 p_1 = 1 \quad \text{with} \quad p_i = e^{-2K_i} \, . \tag{14}$$

Moving to a smooth triangulation of the 2-sphere introducing equilateral triangles on each of the 20 faces of the Icosahedron projecting radially unit 3-vectors $\vec{r}_i$ in $\mathbb{R}^3$ as illustrated in Fig.4. The result is smooth but non-uniform triangulation of the sphere that in the continuum limit approaches an affine map to each tangent plane. We introduce a nearest neighbor Ising model on the triangular lattice,

$$S_{\mathbb{S}^2} = -\sum_{\langle i,j \rangle} K_{ij} s_i s_j \quad \text{with} \quad \sinh(2K_{ij}) = \frac{\ell_{ij}^*}{\ell_{ij}} \, , \tag{15}$$

with coupling constraint form as you approach the continuum locally on each tangent plane as a function of the edge lengths, $\ell_{ij} = |\vec{r}_i - \vec{r}_j|$, and its circumcenter dual lengths, ℓ_{ij}^*, perpendicular to the edge $\langle i,j \rangle$. The Icosahedron has 120 element Icosahedron subgroup I_h of $O(3)$, which is respected by our *naive* icosahedral projecting and our subsequent equal area refinement (16).
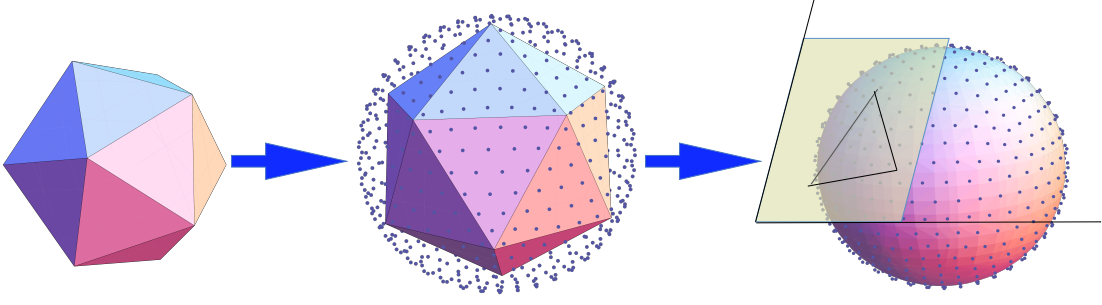
Figure 4: Steps in the basic discretization of $\mathbb{S}^2$ using an icosahedral base refining– shown here for a refinement of L = 3 into L^2 triangle on each of the 20 icosahedral faces, subsequently projected onto the sphere. The Euler condition, $N - E + F = 2$, is satisfied for $N = 2 + 10L^2$ (sites) , $E = 30L^2$ (edges) and $F = 20L^2$ (faces).

4. Numerical Test on $\mathbb{S}^2$

As a comparison we recall earlier we introduce counter terms, for the $\lambda_0 \phi^4$ theory to remove the non-uniform UV cut-off on the triangulated sphere. The kinetic term (7) is unchanged for the FEM form,$K_{ij} = \ell_{ij}^*/\ell_{ij}$, which is exact for the free theory ($\lambda_0 = 0$). The FEM form is modified by locally mass shift by $\delta m_i^2 = \lambda_0 \log(a^2/a_i^2)$ by numerically computing the one loop the UV divergent diagram on the triangulated sphere. Even at $\lambda_0 = 1$ Monte Carlos simulations gave remarkably accurate results on both are $\mathbb{S}^2$ and with similar 3d counter terms on $\mathbb{R} \times \mathbb{S}^2$. Further analysis demonstrated that in the continuum limit the bare coupling must be scaled to zero holding the renormalized coupling $\lambda_R \sim \lambda_0/a^2$ fixed.

Where as for the Ising model we used coupling constants, $\sinh(2K_{ij}) = \ell_{ij}^*/\ell_{ij}$, consistent with the $\lambda_0 = \infty$ The result is a UV critical theory with only nearest neighbor coupling and NO counter terms. Testing restoration of spherical symmetry for the two point function is given in Fig.5.
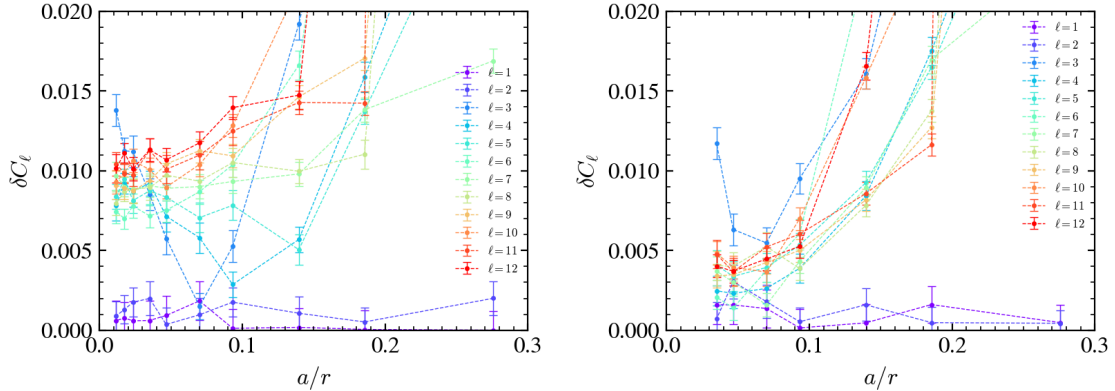

Figure 5: Breaking of rotational symmetry using the basic icosahedral discretization of S^2. On the left for the Ising module vs on the right for the critical ϕ^4 theory with local perturbative counter-terms

We note that our critical Ising map on the left in Fig. 5 is if anything **worse** than for ϕ^4 theory with perturbative counter term? **What is wrong?** Typically the FEM for the Regge manifold

is very forgiving. Any reasonable smooth triangulation of the sphere approaches the continuum manifold and with care a differential metric. BUT our tests presumed that we converge to the "right co-ordinate system" for the Ylm projection. A plausible criterion is to force the curvature defect ϵ_h to have equal weights approaching smooth density in the continuum. In Ref. [19] it was proven that on $\mathbb{S}^d$ ϵ_h is proportional dual areas for the hing approach $\mathbb{S}^d$.

To accomplish this, we vary the edge length ℓ_{ij} to minimize the squared area of the triangle $A_\triangle(i^*)$

$$E_\triangle[\ell_{ij}] = \frac{1}{N}Min[\sum_{i^*=1}^{F} A_\triangle^2(i^*)] \tag{16}$$

labeled by the dual sites $i^* = 1, 2, \cdots, F$ (or F faces) by moving the unit vector $\hat{r}_i$ for position the site. Since the co-ordinates, $\hat{r})i$, have 2N degrees of freedom with $F = 4 + 2N^2$, after removing 3 rotations and one scale, this is 1-1 constrained system for a non-linear [1] ferromagnetic Heisenberg spin system $\vec{S}_i = \hat{r}_i$. Most likely, there is a unique ground state in the continuum as illustrated on the left in Fig. 6. Note if instead we had chosen to minimize the dual $N = 10L^2$ areas, this system would be ill-determine. Fortunately area minimization accomplishes this smoothing of curvature density as a side effect as illustrated on the right in Fig. 6. With area smoothing we now see that
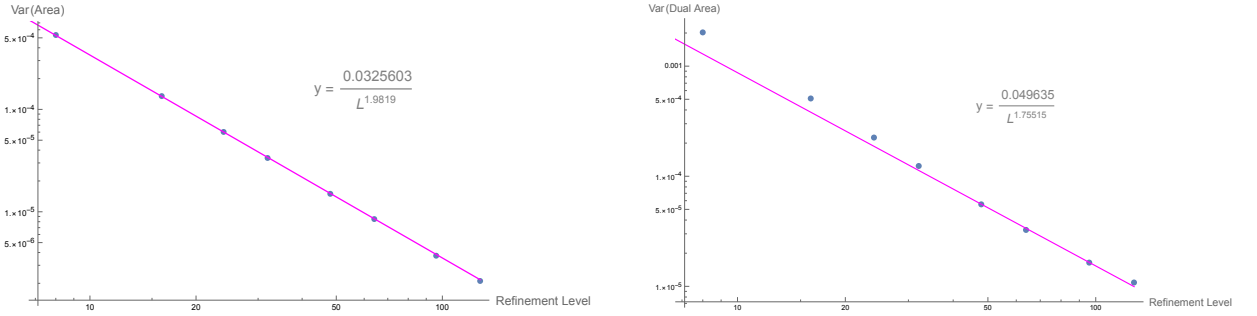

Figure 6: On the left the RMS value of triangle area as the refinement increase and on the right the consequences for the Dual area.

spherical symmetry is improve substantially in Fig.7 on the left and on the right, the fits to the two point function agrees with the exact value with error of 10^{-4} with modest simulations.

With the exact Icosahedral group preserved in our smoothing we are now improving the tests rotational symmetry by imposing this on the Monte Carlo sample

$$\begin{aligned} C_{l_1m_1;l_2m_2} &= \sum_{i,j} \sqrt{g_i}Y_{l_1m_1}^*(\hat{r}_i)\frac{1}{|g|}\sum_{g\in Ih}\langle s(g\hat{r}_i)s(g\hat{r}_j)\rangle\sqrt{g_j}Y_{l_2,m_2}(\hat{r}_j) \\ &\rightarrow c_lP_{l_1}(\hat{r}_i\cdot\hat{r}_j)\delta_{l_1,l_2}\delta_{m_1,m_2} + O(a^2) \end{aligned} \tag{17}$$

---

[1]The area squared using Heron's formula, $16A^2(a,b,c = (a+b+c)(-a+b+c)(a-b+c)(a+b-c)$, with 3 edge lengths $\ell_{ij}^2 = 2 - 2\hat{r}_i\cdot\hat{r}_j$ labeled by a,b,c is 8th order polynomial in the spins.
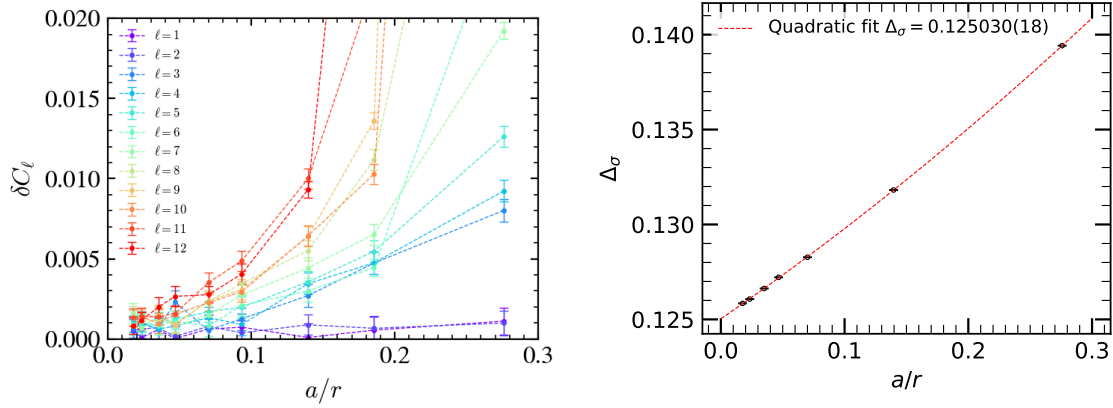
Figure 7: On the left reduced spherical symmetry break approaching the continuum with equal Area co-ordinate smoothing. On the right the Ising Z_2 scalar dimension approaches the exact value $\Delta_\sigma = 1/4$ to $O(10^{-4})$.

a average over the Icosahedral group. This will remove exactly the sampling errors in the IR representation for the $l = 0, 2, 3$ levels visible in Fig. 5 and Fig.7. With higher statistic on lattice with smaller lattices spacing, we believe tests to a $O(10^{-5})$ tolerance are feasible.

5. Next steps

Beyond the 2d Ising model, we are extending our methods to non-integral field theories. First for the 2d ϕ^4 on $\mathbb{S}^2$ lattices and next for 3d Ising and ϕ^4 theory on $\mathbb{R} \times \mathbb{S}^2$ and $\mathbb{S}^3$. Remarkable $\mathbb{S}^3$ has an analogue of the Icosahedral Platonic. The convex regular 4-polytope 600 cell with Schläfli [10] symbol $\{3, 3, 5\}$ or 600 cell with $120^2 = 14400$ elements by embedded un two copies Icosahedral group of $SO(4) = SU(2)_L \times SU(2)_R/Z_2$. To introduce gauge and fermion beyond the FEM form [5] we are implementing $QED3$ with even number of flavors. The question of whether 2 flavor is conformal or not is not yet settled [20]. This is nice 3d analogue to the extension to 4d gauge multi-flavor near conformal BSM theories [21].

In quantum field theory, we know that the Energy Momentum operator is the stress in response to changes in metric stain for correlators:

$$\frac{\delta \langle \phi(x_1)\phi(x_2) \cdots \phi(x_n) \rangle_g}{\delta g^{\mu\nu}(x)} = \langle \phi(x_1)\phi(x_2) \cdots \phi(x_n) T_{\mu\nu}(x) \rangle_g \tag{18}$$

The fundament problem in Euclidean space to lift the stress strain analysis [22] of classical FEM to a quantum critical point. We are considering shifted boundary methods[23] and renormalized Wilson flow operators [24] to design better algorithmic methods and provide a stronger theoretical understanding of the affine map to lattice quantum fields on curved manifolds.

Acknowledgments

References

[1] R.C. Brower and E.K. Owen, *The ising model on* $\mathbb{S}^2$, `2407.00459`.

[2] R.C. Brower and E.K. Owen, *Ising model on the affine plane*, *Phys. Rev. D* **108** (2023) 014511 [`2209.15546`].

[3] T. Regge, *General relativity without coordinates*, *Nuovo Cim.* **19** (1961) 558.

[4] J.L. Cardy, *Universal amplitudes in finite-size scaling: generalisation to arbitrary dimensionality*, *J. Phys. A* **18** (1985) L757.

[5] R.C. Brower, G.T. Fleming, A.D. Gasbarro, T.G. Raben, C.-I. Tan and E.S. Weinberg, *Lattice Dirac Fermions on a Simplicial Riemannian Manifold*, *Phys. Rev.* **D95** (2017) 114510 [`1610.08587`].

[6] R.C. Brower, M. Cheng, E.S. Weinberg, G.T. Fleming, A.D. Gasbarro, T.G. Raben et al., *Lattice ϕ^4 field theory on Riemann manifolds: Numerical tests for the 2-d Ising CFT on* $\mathbb{S}^2$, *Phys. Rev.* **D98** (2018) 014502 [`1803.08512`].

[7] R.C. Brower, G.T. Fleming, A.D. Gasbarro, D. Howarth, T.G. Raben, C.-I. Tan et al., *Radial lattice quantization of 3D ϕ^4 field theory*, *Phys. Rev. D* **104** (2021) 094502 [`2006.15636`].

[8] V. Ayyar, R.C. Brower, G.T. Fleming, A.-M.E. Glück, E.K. Owen, T.G. Raben et al., *Operator product expansion for radial lattice quantization of 3D ϕ^4 theory*, *Phys. Rev. D* **109** (2024) 114518 [`2311.01100`].

[9] Lüscher, M., *Dimensional Regularization in the Presence of Large Background Fields*, *Annals Phys.* **142** (1982) 359.

[10] R. Kellerhals, *Ludwig Schläfli – an ingenious Swiss mathematician*, *Elemente der Mathematik* **65** (2010) 156.

[11] J.W. Barrett, D. Oriti and R.M. Williams, *Tullio regge's legacy: Regge calculus and discrete gravity*, 2019.

[12] H.W. Hamber and G. Kagel, *Exact Bianchi identity in Regge gravity*, *Class. Quant. Grav.* **21** (2004) 5915 [`gr-qc/0107031`].

[13] Seramika Ariwahjoedi and Freddy P. Zen, *(2+1) Regge Calculus: Discrete Curvatures, Bianchi Identity, and Gauss-Codazzi Equation*, `1709.08373`.

[14] S. Ariwahjoedi and F.P. Zen, *Contracted Bianchi Identity and Angle Relation on n-dimensional Simplicial Complex of Regge Calculus*, `1807.11420`.

[15] W.A. Miller, J.R. McDonald, P.M. Alsing, D. Gu and S.-T. Yau, *Simplicial Ricci Flow*, *Commun. Math. Phys.* **329** (2014) 579 [`1302.0804`].

[16] G. Perelman, *Ricci flow with surgery on three-manifolds*, `math/0303109`.

[17] J.W. Morgan and G. Tian, *Ricci flow and the poincare conjecture*, math/0607607.

[18] U. Wolff, *Ising model as Wilson-Majorana Fermions*, *Nucl. Phys. B* **955** (2020) 115061 [2003.01579].

[19] G. Feinberg, R. Friedberg, T.D. Lee and H.C. Ren, *Lattice Gravity Near the Continuum Limit*, *Nucl. Phys.* **B245** (1984) 343.

[20] N. Karthik and R. Narayanan, *Scale-invariance of parity-invariant three-dimensional QED*, *Phys. Rev. D* **94** (2016) 065026 [1606.04109].

[21] R.C. Brower, A. Hasenfratz, C. Rebbi, E. Weinberg and O. Witzel, *Composite Higgs model at a conformal fixed point*, *Phys. Rev. D* **93** (2016) 075028 [1512.02576].

[22] L.D. Landau and E.M. Lifshitz, *Theory of Elasticity*, Pergamon Press, Oxford, 3rd ed. (1986).

[23] L. Giusti and H.B. Meyer, *Thermodynamic potentials from shifted boundary conditions: the scalar-field theory case*, *JHEP* **11** (2011) 087 [1110.3136].

[24] C. Monahan and K. Orginos, *Locally smeared operator product expansions in scalar field theory*, *Phys. Rev. D* **91** (2015) 074513 [1501.05348].